2017 IEEE Conference on Control Technology and Applications (CCTA)
August 27-30, 2017. Kohala Coast, Hawai'i, USA

Harmonic Reduction via Optimal Power Flow and the Frequency Coupling Matrix

Yanhua Tian
University of Toronto, Canada

Na Li
Harvard University, USA

Joshua A. Taylor
University of Toronto, Canada

***Abstract*— In this paper we propose a new optimal power flow scheme that takes into account the harmonics generated by power electronics interfaced distributed generation (DG). The objective is to minimize the cost of generation under constraints on the total harmonic distortion (THD) of voltage. The frequency coupling matrix (FCM) is used to model the harmonic current injected by a converter. Network current and voltage are modeled for each harmonic frequency. Constraints limiting the maximum voltage THD are introduced to the three-phase optimal power flow (OPF) problem. We construct a semidefinite relaxation, which can be solved using commercially available software packages. We give numerical results for the harmonic-constrained optimal power flow for two test systems.**

I. Introduction

Incorporating renewable distributed generations (DG) into a power network can reduce generation costs and improve reliability [1], [2]. Optimal power flow (OPF) is used to minimize the cost of generation subject to system constraints [3]. Though the nominal OPF is non-convex and hence hard to solve, semidefinte relaxation (SDR) can approximate OPF as a convex semidefinite program [4]. However, the standard OPF omits the harmonics introduced into the network by power electronic-interfaced DGs and non-linear loads. Excessive harmonics can increase conductor heating loss, cause transformer derating and power quality issues [5], [6]. The frequency coupling matrix (FCM) is a popular approach to modeling the coupling between an individual converters voltage and current harmonics [7], [8]. The value of the FCM can be calculated either from piecewise linear differential equations or field measurements [9], [10]. To date, FCM-based approaches have not been used to incorporate harmonics in OPF.

In this paper, we develop a new framework that minimizes the cost of generation while maintaing voltage harmonic distortions beneath a specified level. The proposed harmonic-constrained optimal power flow (HC-OPF) is novel in the following regards:

- Inclusion of the FCM model for each power electronic converter. The FCM of a converter links its harmonic current injection and the voltage harmonics at the point of common coupling in the network.
- Construction of network and load impedance models at harmonic frequencies, and the modeling of network voltage and current harmonics.
- Constraints limiting the network harmonic voltage in terms of the total harmonic distortion (THD).

TABLE I
NOMENCLATURE

$\mathcal{N}$	Set of nodes in the microgrid
ε	Set of distribution lines in the microgrid
$\mathcal{S}$	Set of nodes featuring DG
$\mathcal{N}_{n,\phi}$	Set of neighbouring nodes of $n \in \mathcal{N}$ that also contain phase ϕ
$\mathcal{P}_n$	Set of the phases at node n
$\mathcal{P}_{mn}$	Set of the phases of line (m,n)
$V_{n,\phi}$	Complex line-to-ground voltage at phase ϕ of node n
$I_{n,\phi}$	Complex current injection at phase ϕ of node n
$I_{mn,\phi}$	Complex current on phase ϕ of line (m,n)
$P_{L,n,\phi}$	Active load demanded at node n on phase ϕ
$Q_{L,n,\phi}$	Reactive load demanded at node n on phase ϕ
$P_{G,n,\phi}$	Active power supplied at node n on phase ϕ
$Q_{G,n,\phi}$	Reactive power supplied at node n on phase ϕ
$P_{mn,\phi}$	Active power exiting phase ϕ of node m on line (m,n)
$Q_{mn,\phi}$	Reactive power exiting phase ϕ of node m on line (m,n)
$\mathbf{Z}_{mn}$	Phase impedance matrix of line (m,n)
$\mathbf{Y}_{s,mn}$	Shunt admittance matrix of line (m,n)
$\underline{V}_n$, $\overline{V}_n$	Voltage magnitude lower (upper) limit at nodes of $n \in \mathcal{N}$
$\underline{P}_{G,s,\phi}$, $\overline{P}_{G,s,\phi}$	Minimum (Maximum) active power supplied at phase ϕ of node $s \in \mathcal{S}$
$\underline{Q}_{G,s,\phi}$, $\overline{Q}_{G,s,\phi}$	Minimum (Maximum) reactive power supplied at phase ϕ at node $s \in \mathcal{S}$

The new framework is based on a three-phase unbalanced OPF [11], which accommodates with both single-phase and three-phase power electronic converters. We use SDR to obtain a semidefinite relaxation, in which power flow and total harmonic distortion constraints are convex. Numerical tests demonstrate that the proposed framework can find OPF solutions satisfying a network harmonic distortion limit.

This paper is organized as follows. Section II provides the background about the three phase load flow problem and the FCM. In section III we propose a framework that combines the FCM with three phase load flow to analyze harmonics across the network. Section IV gives the harmonic-constrained OPF problem and its relaxation. Section V presents the numerical result for solving the problem on a 10-bus test network and IEEE 13-bus feeder. Section VI is the conclusion. The notation used in this paper is listed in Table I.

978-1-5090-2182-6/17/$31.00 ©2017 IEEE

II. Background

A. Three-Phase Load Flow

Distribution networks are unbalanced by nature. Consequently, all three phases should be included in the model of a load flow problem. We denote the nodes $\mathcal{N} = \{0, 1, \cdots, N\}$ and edges $\varepsilon \subseteq \mathcal{N} \times \mathcal{N}$ connecting pairs of nodes. DGs are connected to the network at a subset of nodes $\mathcal{S}$. Each node $n \in \mathcal{N}$ is connected to a subset of phases $\mathcal{P}_n \subseteq \{a, b, c\}$. Let $V_{n,\phi}$ and $I_{n,\phi} \in \mathbb{C}$ be the line-to-ground voltage and injected current of phase $\phi \in \mathcal{P}_n$ at node n. Active and reactive load at a node n are specified for each phase ϕ as $P_{L,n,\phi}$ and $Q_{L,n,\phi}$ respectively. Similarly, $P_{G,n,\phi}$ and $Q_{G,n,\phi}$ are the active and reactive power injection of the generator if a DG is connected to node n, i.e. $n \in \mathcal{S}$.

Each edge $mn \in \varepsilon$ represents a distribution line or cable connecting a set of phases $\mathcal{P}_{mn} \subseteq \mathcal{P}_m \cap \mathcal{P}_n$ from node m to n. The line is modeled as a π network and characterized by its phase impedance and shunt admittance matrices $\mathbf{Z}_{mn}, \mathbf{Y}_{s,mn} \in |\mathcal{P}_{mn}| \times |\mathcal{P}_{mn}|$ [12]. Because the system is unbalanced, these matrices are typically not diagonal. Denoting the complex current flow from node m to n as $\mathbf{I}_{mn} = \{I_{mn,\phi} |\ \phi \in \mathcal{P}_{mn}\}$, Ohm's Law is given by:

$$\mathbf{I_{mn}} = \mathbf{Z}_{mn}^{-1}([\mathbf{V_m}]_{\mathcal{P}_{mn}} - [\mathbf{V_n}]_{\mathcal{P}_{mn}}), \quad mn \in \varepsilon. \quad (1)$$

The notation $[\mathbf{V}]_{\mathcal{P}_{mn}}$ denotes the sub-vector of $\mathbf{V}$ that only contains elements of the phases in the line mn, i.e. $[\mathbf{V_m}]_{\mathcal{P}_{mn}}, [\mathbf{V_n}]_{\mathcal{P}_{mn}} \in \mathbb{C}^{|\mathcal{P}_{mn}|}$. In addition, Kirchoff's Current Law (KCL) holds at each node and phase:

$$I_{n,\phi} = \sum_{m \in \mathcal{N}_{n,\phi}} \Bigg[\left(\frac{1}{2} \mathbf{Y_{s,mn}} + \mathbf{Z_{mn}}^{-1} \right) [\mathbf{V_n}]_{\mathcal{P}_{mn}} - \mathbf{Z_{mn}}^{-1} [\mathbf{V_m}]_{\mathcal{P}_{mn}} \Bigg]_{\phi}, \quad \forall n \in \mathcal{N}, \quad \phi \in \mathcal{P}_n, \quad (2)$$

where $\mathcal{N}_{n,\phi}$ is the set of neighbouring bus of node n that also include ϕ in its available phases, and the subscript $[\cdot]_\phi$ denotes the elements of the bracketed vector corresponding to phase ϕ. KCL and Ohm's Law for all nodes in the system can be written in matrix form as:

$$\mathbf{I} = \mathbf{YV}, \quad (3)$$

where $\mathbf{Y}$ is the system admittance matrix and $\mathbf{V}$, $\mathbf{I} \in \mathbb{C}^{\sum_{n=0}^{N} |\mathcal{P}_n|}$ are system node voltage vector and current injection vector:

$$\mathbf{V} = [V_{0,a},\ V_{0,b},\ V_{0,c},\ \cdots\ V_{N,b}, V_{N,c}]^T$$
$$\mathbf{I} = [I_{0,a},\ I_{0,b},\ I_{0,c},\ \cdots\ I_{N,b}, I_{N,c}]^T.$$

We follow the convention that $P_{G,n,\phi} = Q_{G,n,\phi} = 0$ if $n \in \mathcal{N} \setminus \mathcal{S}$. The total power injection into the network at a node is given by:

$$V_{n,\phi} {I_{n,\phi}}^* = \left(P_{G,n,\phi} - P_{L,n,\phi} \right) + j \left(Q_{G,n,\phi} - Q_{L,n,\phi} \right) \quad \forall \phi \in \mathcal{P}_n,\ n \in \mathcal{N}. \quad (4)$$

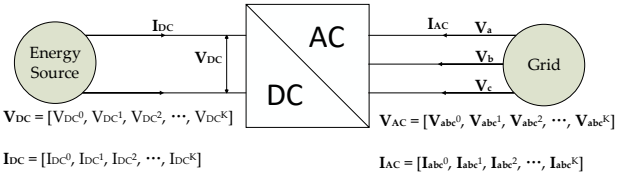

Fig. 1. Power Electronics Interfaced DG

We designate one node in the network as the slack bus and and fix its voltage to one per unit. Often the Point of Common Coupling (PCC) where the distribution network is connected to the transmission network is set to be the slack bus and its voltage is set to be $[V_{0,a},\ V_{0,b},\ V_{0,c}] = \left[e^{0j},\ e^{\frac{-2\pi}{3}j},\ e^{\frac{2\pi}{3}j}\right]$ per unit. For a given load $\{P_{L,n,\phi}, Q_{L,n,\phi}\}$ and generator input $\{P_{G,s,\phi}, Q_{G,s,\phi}\}$, the voltage value at each bus is determined by equations (3) and (4).

B. Frequency Coupling Matrix

Traditionally, converter harmonics are modeled as a fixed current source with a harmonic spectrum. However, this model fails to capture the additional harmonic currents generated by harmonic voltage present at the PCC. From a network perspective, the harmonic current injected by an individual converter distorts the voltage profile across the network, and in turn impacts the harmonic current injection of other converters. This coupling between harmonic voltage and current cannot be captured by a fixed current source model. The frequency coupling matrix of a converter models its admittance at harmonic frequencies and the cross-coupling of different harmonics.

Fig. 1 shows a DG connected to the grid via a three-phase converter. The FCM of a converter linearly relates its AC-side current with its AC-side voltage and DC-side current, where each voltage and current vector contains elements of both the fundamental and harmonic frequencies up to any desired order. The FCM of a voltage source converter (VSC) using Pulse Width Modulation (PWM) can be mathematically derived from its parameters as in [9], or experimentally measured as in [10].

In [9], each time-domain signal is decomposed into its Fourier series and represented by its fundamental and harmonic phasors, which exist in conjugate pairs for each harmonic order k and $-k$ according to Euler's equation:

$$f(t) = f_0 + \sum_{n=1}^{\infty} a_n \cos(n\omega t) + b_n \sin(n\omega t)$$
$$= f_0 + \sum_{n=1}^{\infty} c_n e^{jn\omega t} + c_n^* e^{-jn\omega t}$$

Since the harmonic components of the converter DC-side current I_{dc} are negligible [9], the FCM for a converter can

be approximated as:

$$\mathbf{I_{ac}} = \left[\mathbf{FCM}\right] \begin{bmatrix} \mathbf{V_{ac}} \\ I_{dc} \end{bmatrix}. \tag{5}$$

In (5), $\mathbf{I_{ac}} = \left[I^{-K}, \cdots, I^{K}\right]^T$ and $\mathbf{V_{ac}} = \left[V^{-K}, \cdots, V^{K}\right]^T$ for a single-phase converter. $\mathbf{I_{ac}} = \left[I_a^{-K}, \cdots, I_a^K, I_b^{-K}, \cdots, I_b^K, I_c^{-K}, \cdots, I_c^K\right]^T$ and $\mathbf{V_{ac}} = \left[V_a^{-K}, \cdots, V_a^K, V_b^{-K}, \cdots, V_b^K, V_c^{-K}, \cdots, V_c^K\right]^T$ for a three-phase converter. The size of the FCM depends on the maximum harmonic order K, which is a design parameter of the FCM. Also $I^{-n} = I^{n*}$ and $V^{-n} = V^{n*}$. The FCM in the above equations can be calculated when the parameters of the converter are known [9].

Our objective is to use the FCM to link the harmonics with fundamental voltage and power quantities. To facilitate this, we make the following modifications to equation (5).

- A converter's FCM over its operating range is approximated as a constant, and calculated when the converter is injecting its rated power into the network via nominal PCC voltage.
- Since converters in power systems are intended to primarily generate fundamental frequency voltage and current, the impact of higher order harmonics on the fundamental frequency current is neglected.
- The FCMs are reformulated into three parts that are associated with the fundamental frequency voltage, harmonic frequency voltage and DC current respectively.
- If the DC-side voltage V_{DC} of a VSC is well regulated[13], and the conversion losses of the converter are negligible, the DC-side current I_{DC} can be replaced with its AC-side power injection by dividing the associated entries of FCM by V_{DC}.
- Since the harmonic voltage and current are regulated to be smaller than the fundamental frequency components, the total power consumed by the converter is approximated by its power injection at the fundamental frequency, P^1.

With these modifications, equations (5) can be re-formulated as:

$$\mathbf{I_h} = \left[\mathbf{K_V}\right] \begin{bmatrix} {V^1}^* \\ V^1 \end{bmatrix} + \left[\mathbf{K_P}\right] P^1 + \left[\mathbf{K_{V_h}}\right] \begin{bmatrix} {\mathbf{V_h}}^* \\ \mathbf{V_h} \end{bmatrix} \tag{6}$$

$$\begin{bmatrix} \mathbf{I_{ah}} \\ \mathbf{I_{bh}} \\ \mathbf{I_{ch}} \end{bmatrix} = \left[\mathbf{K_V}\right] \begin{bmatrix} {V_a^1}^* \\ {V_b^1}^* \\ {V_c^1}^* \\ V_a^1 \\ V_b^1 \\ V_c^1 \end{bmatrix} + \left[\mathbf{K_P}\right] P^1 + \left[\mathbf{K_{V_h}}\right] \begin{bmatrix} {\mathbf{V_{ah}}}^* \\ {\mathbf{V_{bh}}}^* \\ {\mathbf{V_{ch}}}^* \\ \mathbf{V_{ah}} \\ \mathbf{V_{bh}} \\ \mathbf{V_{ch}} \end{bmatrix}, \tag{7}$$

where the vectors with subscript h contain harmonic components, and for a three-phase converter P^1 is the sum of the fundamental frequency power injection of all three phases:

$$\mathbf{I_h} = \left[I^0 \ I^2 \ \cdots \ I^K\right]^T$$
$$\mathbf{I_{ah}} = \left[I_a^0 \ I_a^2 \ \cdots \ I_a^K\right]^T$$
$$P^1 = P_a^1 + P_b^1 + P_c^1.$$

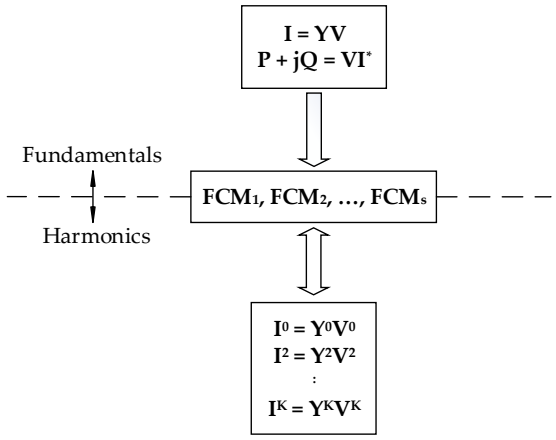

Fig. 2. Framework for Network Harmonics Analysis

The modified harmonic model (6) and (7) capture the dependence of the harmonic current injection $\mathbf{I_h}$ on the fundamental frequency power flow solution (V^1 and P^1), as well as voltage harmonics $\mathbf{V_h}$ present at the converter terminal.

III. Network Harmonics Model

In this section, we propose a framework for analyzing the harmonics across the network by combining the fundamental power flow analysis and converter FCM models. In this analysis, generator power injection and load values are taken as input and nodal voltage and current injection at fundamental and harmonic frequencies are solved as output. We also provide a numerical example on a three-bus test system.

A. Modeling

Our model contains two parts: for each harmonic order a new impedance network is constructed to model harmonic current flow at that frequency; and for each converter in the network, its FCM is employed to couple its harmonic current injection with its terminal harmonic voltage and the fundamental power flow solution.

First, additional notations and variables are defined. Let K be the maximum order harmonic in the model. This is also the dimension of the FCM specified for each converter. Harmonic voltage vector $\mathbf{V_h} \in \mathbb{C}^{K\sum_{n=1}^{N}|\mathcal{P}_n|}$ is defined in terms of the vector $\mathbf{V_{n,\Phi h}} \in \mathbb{C}^{K|\mathcal{P}_{n,\phi}|}$ at individual node n

and phase ϕ as follows:

$$\mathbf{V_h} = \begin{bmatrix} \mathbf{V_{0,ah}} \\ \mathbf{V_{0,bh}} \\ \mathbf{V_{0,ch}} \\ \vdots \\ \mathbf{V_{N,bh}} \\ \mathbf{V_{N,ch}} \end{bmatrix} \qquad \mathbf{V_{n,\Phi h}} = \begin{bmatrix} V_{n,\phi}^0 \\ V_{n,\phi}^2 \\ V_{n,\phi}^3 \\ \vdots \\ V_{n,\phi}^K \end{bmatrix}.$$

Let $\mathcal{S}_\Phi \subseteq \{(n,\phi)|n \in \mathcal{N}, \phi \in \mathcal{P}_n\}$ be the set of node and associated phase pairs where single-phase DGs are connected into the distribution network. Let $\mathcal{S}_{3\Phi}$ be the sets of nodes where three-phase DGs are installed in the distribution network. By definition each node in $\mathcal{S}_{3\Phi}$ contains all three phases. The harmonic current injection and terminal voltage for each DG in the network can be modeled via its FCM as follows:

$$\mathbf{I_{G,n,\Phi h}} = \left[\mathbf{K_{V,n\Phi}}\right] \begin{bmatrix} {V_{n,\phi}}^* \\ V_{n,\phi} \end{bmatrix} + \left[\mathbf{K_{P,n\Phi}}\right] P_{G,n,\phi} + \left[\mathbf{K_{V_{h,n\Phi}}}\right] \begin{bmatrix} \mathbf{V_{n,\Phi h}}^* \\ \mathbf{V_{n,\Phi h}} \end{bmatrix} \quad \forall (n,\phi) \in \mathcal{S}_\Phi \quad (8)$$

$$\begin{bmatrix} \mathbf{I_{G,n,ah}} \\ \mathbf{I_{G,n,bh}} \\ \mathbf{I_{G,n,ch}} \end{bmatrix} = \left[\mathbf{K_{V,n}}\right] \begin{bmatrix} {V_{n,a}}^* \\ {V_{n,b}}^* \\ {V_{n,c}}^* \\ V_{n,a} \\ V_{n,b} \\ V_{n,c} \end{bmatrix} + \left[\mathbf{K_{P,n}}\right] P_{G,n,abc} + \left[\mathbf{K_{V_{h,n}}}\right] \begin{bmatrix} \mathbf{V_{n,ah}}^* \\ \mathbf{V_{n,bh}}^* \\ \mathbf{V_{n,ch}}^* \\ \mathbf{V_{n,ah}} \\ \mathbf{V_{n,bh}} \\ \mathbf{V_{n,ch}} \end{bmatrix} \quad \forall n \in \mathcal{S}_{3\Phi} \quad (9)$$

Similar to (1) and (2), Ohm's Law for each line and KCL at each bus can be used to form a model at each harmonic frequency:

$$\mathbf{I_{mn}^k} = (\mathbf{Z_{mn}^k})^{-1} \left([\mathbf{V_m^k}]_{\mathcal{P}_{mn}} - [\mathbf{V_n^k}]_{\mathcal{P}_{mn}}\right) \quad \forall (m,n) \in \mathcal{E} \quad k = \{0,2,\cdots,K\} \quad (10)$$

$$I_{n,\phi}^k = \sum_{m \in \mathcal{N}_{n,\phi}} \left[\left(\frac{1}{2} \mathbf{Y_{s,mn}^k} + (\mathbf{Z_{mn}^k})^{-1} \right) [\mathbf{V_n^k}]_{\mathcal{P}_{mn}} - (\mathbf{Z_{mn}^k})^{-1} [\mathbf{V_m^k}]_{\mathcal{P}_{mn}} \right]_\phi \quad \forall n \in \mathcal{N},\ \phi \in \mathcal{P}_n,\ k = \{0,2,\cdots,K\} \quad (11)$$

In the above equations, $\mathbf{Z_{mn}^k}$ and $\mathbf{Y_{s,mn}^k}$ indicates the matrix at harmonic frequency k. The exact values of these matrices are not available from the standard specifications. We extrapolate these values by scaling the reactive components based on the new frequency: $X_L(\omega) = j\omega L$ and $X_C(\omega) = \frac{1}{j\omega C}$. Voltage variable $\mathbf{V_n^k} \in \mathbb{C}^{|\mathcal{P}_n|}$ and $\mathbf{V_m^k} \in \mathbb{C}^{|\mathcal{P}_m|}$ are constructed by collecting the k-th order harmonic voltage terms at buses n and m. Equivalently, KCL of all the nodes in the system at harmonic order k can be compactly written in matrix form as:

$$\mathbf{I}^k = \mathbf{Y}^k \mathbf{V}^k, \quad (12)$$

where $\mathbf{Y}^k$ is the network admittance matrix at harmonic frequency $k\omega$. $\mathbf{V}^k$ and $\mathbf{I}^k$ are the system node voltage vector and current injection vector for harmonic order k respectively. Unlike the case for fundamental frequency, no loads are specified at harmonic frequencies, which eliminates the needs for additional power flow constraints similar to (4).

Load modelling at harmonic frequencies has been studied by many researchers [14]–[16]. Two types of load are considered: linear load and non-linear load. Linear load are passitive and do not generate additional harmonics while non-linear load similar to converters are harmonic sources.

The behavior of various types of linear load (constant power, constant impedance and constant current) at harmonic frequencies are different. However, in each case an equivalent RLC circuit model is typically constructed based on the load decomposition and harmonic frequency. In this study, we model a linear load of power $P_{L,n,\phi}$ and $Q_{L,n,\phi}$ connected at bus n of phase ϕ as an RL impedance approximated by:

$$Z_{L,n,\phi} = \frac{V_0^2}{P_{L,n,\phi} + Q_{L,n,\phi} j} = R_{L,n,\phi} + jX_{L,n,\phi}$$

V_0 is the nominal operating voltage for the load, i.e. $V_0 = 1$ per unit. The load impedance also varies with frequency and can be approximated as:

$$Z_{L,n,\phi}^k = R_{L,n,\phi} + jkX_{L,n,\phi}$$

For each harmonic frequency order k, construct the diagonal load admittance matrix $\mathbf{Y_L^k}$ as follows:

$$\mathbf{Y_L^k} = \text{diag}\left\{(Z_{L,0,a}^k)^{-1}, (Z_{L,0,b}^k)^{-1}, \cdots, (Z_{L,N,c}^k)^{-1}\right\}$$

Then $\mathbf{Y_L^k V^k}$ will be the vector of k-th order harmonic current absorbed by linear load in the network:

$$\mathbf{I_{LL,}^k} = \mathbf{Y_L^k V^k} \quad (13)$$

Denote the current vector $\mathbf{I_{NLL}^k}$ as the k-th order harmonic current generated by the non-linear load in the system, it can be modeled in two ways. The simplest way is considering it as a constant harmonic current source $\mathbf{I_{NLL,n,\Phi h}} = \left[I_{NLL,n,\phi}^0,\ I_{NLL,n,\phi}^2, \cdots, I_{NLL,n,\phi}^K\right]^T$. If the harmonic current generated by the non-linear load is variable, its harmonic characteristics is similar to that of a DG and can be modeled by its FCM. In that case the coupling between $\mathbf{I_{NLL,n,\Phi h}}$ and $\mathbf{V_{n,\Phi h}}$ can be described in the same form as equation (8) and (9) for single-phase and three-phase non-linear load respectively.

When combining current injected by DGs, linear load and linear load, equation (12) can be re-written as:

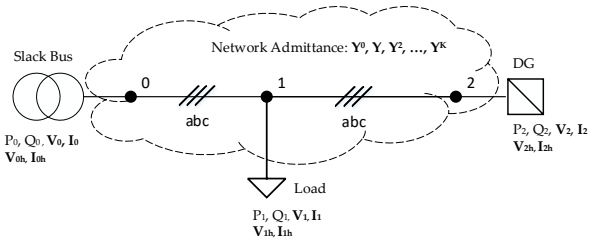

Fig. 3. Network Harmonics Aanlysis Test System

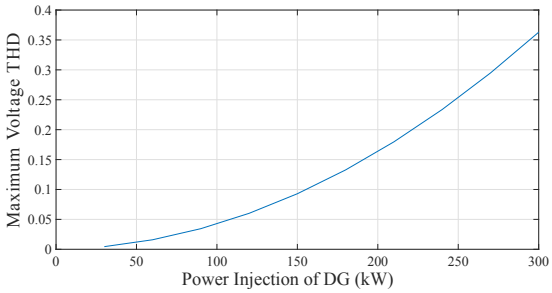

Fig. 4. Network Harmonics Analysis Result: Maximum Voltage THD Value vs. Increasing DG Power Input

$$\mathbf{I}_{\mathbf{G}}^{k} - \mathbf{I}_{\mathbf{LL}}^{k} - \mathbf{I}_{\mathbf{NLL}}^{k} = \mathbf{Y}^{k}\mathbf{V}^{k}, \tag{14}$$

or equivalently:

$$\mathbf{I}_{\mathbf{G}}^{k} - \mathbf{I}_{\mathbf{NLL}}^{k} = \left(\mathbf{Y}^{k} + \mathbf{Y}_{\mathbf{L}}^{k}\right)\mathbf{V}^{k} \tag{15}$$

In summary, the power flow solution along with the converter FCMs provide a boundary condition at the point where the converter is connected. They also provide the coupling from the fundamental to all the harmonics. In addition, the current flow across the network is modeled for every harmonic frequency based on the line admittance and load impedance at that frequency. Any non-linear load is considered a fixed harmonic current source or modeled as a converter with its own FCM. The structure described above is illustrated in Fig. 2. The fundamental frequency load and generator power variables $\mathbf{P}$ and $\mathbf{Q}$ are considered as input to our problem and fundamental and harmonic voltage and current variables $\mathbf{V}$, $\mathbf{I}$, $\mathbf{V_h}$ and $\mathbf{I_h}$ are solved as output.

B. An example of harmonic analysis

In this section, we apply our framework on a three-bus test system. Fig. 3 shows the schematic of the network with variables associated with each bus marked beside it. This is a radial network with three buses rated at 4.16 kV. Each bus contains all three phases. The line impedances are all set to $\mathbf{Z_{mn}} = [0.0347 + j0.1018, 0.0156 + j0.0502, 0.0158 + j0.0424; 0.0156 + j0.0502, 0.0338 + j0.1048, 0.0154 + j0.0385; 0.0158 + j0.0424, 0.0154 + j0.0385, 0.0341 + j0.1035]$. Bus $\#0$ is the slack bus. A load of 100 kW+80 kVAR is connected at each phase of bus $\#1$. A DG is connected to bus $\#2$ via a converter whose parameters are listed in Table II. The FCM of the converter is computed according to [9] with maximum harmonic frequency order $K = 10$.

To quantify the amount of harmonic present in the network, we use the voltage total harmonic distortion (THD) as a metric. THD is typically defined as the sum of the squared harmonic magnitudes normalized by the magnitude of the fundamental frequency:

$$\text{THD}_{n,\phi} = \frac{\sum_{k=0,2,\cdots,K} V_{n,\phi}^{k^2}}{V_{n,\phi}^{2}} \quad \forall n \in \mathcal{N},\ \phi \in \mathcal{P}_n$$

In this example we vary the amount of power generated by the DG from 10 kW to 100 kW, and solve the three-phase load flow for each case using the Newton-Raphson method. The solution is then used as input for the network harmonics analysis. The maximum voltage THD in the network is plotted with respect to the DG generation in Fig. 4. The plot illustrates the impact of DG generation on network harmonics. As shown in the figure the maximum voltage THD increases when more power is generated by the power electronic-interfaced DG.

IV. Harmonic-Constrained Optimal Power Flow

In this section, we describe the harmonic-constrained OPF problem and its SDP relaxation. First the non-convex problem is formed by combining the network harmonic model with a regular OPF problem; then the problem is relaxed to a semidefinite program.

A. Problem Formulation

For a given load $\{P_{L,n,\phi}, Q_{L,n,\phi}\}$, the OPF determines the power injection of each generator $\{P_{G,s,\phi}, Q_{G,s,\phi}\}$ in order to minimize the operating cost of the system. Typical choices of this function are the cost of generation or the total loss in the network. For this study, the cost of power generation is used. In addition to equations (3) and (4), which describe the physical laws governing current and power flow, safety and reliability constraints are imposed to restrict the voltage and DG power injection values within the acceptable limits:

$$\underline{V}_n \leq |V_{n,\phi}| \leq \overline{V}_n \qquad \forall \phi \in \mathcal{P}_n,\ n \in \mathcal{N} \tag{16}$$

$$\underline{P}_{G,s,\phi} \leq P_{G,s,\phi} \leq \overline{P}_{G,s,\phi} \qquad \forall \phi \in \mathcal{P}_s,\ s \in \mathcal{S} \tag{17}$$

$$\underline{Q}_{G,s,\phi} \leq Q_{G,s,\phi} \leq \overline{Q}_{G,s,\phi} \qquad \forall \phi \in \mathcal{P}_s,\ s \in \mathcal{S}. \tag{18}$$

Next, we add harmonic constraints to mitigate the adverse effects of harmonics across the network. From Section III, equations (8), (9) and (15) are included to model the harmonic current flow across the network. To restrict the harmonic effect, the voltage total harmonic distortion is constrained by an upper limit α, or equivalently:

$$\sum_{k=0,2,\cdots,K} V_{n,\phi}^{k^2} \leq \alpha V_{n,\phi}^{2} \quad \forall n \in \mathcal{N},\ \phi \in \mathcal{P}_n \tag{19}$$

In summary, the harmonic-constrained OPF problem is as follows:

(P1)

$$\begin{aligned} \underset{\{\mathbf{P_G},\ \mathbf{Q_G},\ \mathbf{V},\ \mathbf{V_h}\}}{\text{Minimize:}} \quad & C_0 = \sum_{s\in\mathcal{S}} c_s \sum_{\phi\in\mathcal{P}_s} P_{G,s,\phi} \\ \text{Subject to:} \quad & (3),(4),(16),(17),(18) \\ & (8),(9),(15),(19) \end{aligned}$$

This problem is non-convex because of constraints (4), (16) and (19). In the next section, we will apply a semidefinite relaxation to make this problem convex.

B. Semidefinite Relaxation

Semidefinite relaxation is a powerful technique for approximating non-convex quadratically constrained problems like OPF [4], [17]. We now apply this relaxation to the harmonic-constrained OPF.

Consider a rank 1 positive-semidefinite matrix $\mathbf{W} = \mathbf{V}\mathbf{V}^*$. Element $W_{i,j}$ is related to $\mathbf{V}$ as $W_{i,j} = V_i V_j^*$. For each node n and phase ϕ denote the following admittance matrix:

$$\begin{aligned} \mathbf{Y}_{n,\phi} &= \mathbf{e}_{n,\phi}\mathbf{e}_{n,\phi}^*\mathbf{Y} \\ \mathbf{\Phi}_{n,\phi} &= \mathbf{e}_{n,\phi}\mathbf{e}_{n,\phi}^*, \end{aligned}$$

where:

$$\mathbf{e}_{n,\phi} = \left[\mathbf{0}_{|\mathcal{P}_0|}^T, \mathbf{0}_{|\mathcal{P}_1|}^T, \cdots, \mathbf{0}_{|\mathcal{P}_{n-1}|}^T, \mathbf{e}_{|\mathcal{P}_n|}^{\phi,T}, \mathbf{0}_{|\mathcal{P}_{n+1}|}^T, \cdots, \mathbf{0}_{|\mathcal{P}_N|}^T\right]^T$$

and $\mathbf{e}_{|\mathcal{P}_n|}^{\phi}$ denotes the canonical basis of $\mathbb{R}^{|\mathcal{P}_n|}$. Then the non-convex constraints (4), (16) and (19) can be re-written as linear constraints of $\mathbf{W}$ as follows:

$$Tr(\mathbf{Y}_{n,\phi}\mathbf{W}) = \Big(P_{G,n,\phi} - P_{L,n,\phi}\Big) - j\Big(Q_{G,n,\phi} - Q_{L,n,\phi}\Big) \quad \forall \phi \in \mathcal{P}_n,\ n \in \mathcal{N} \quad (20)$$

$$\underline{V_n}^2 \le Tr(\mathbf{\Phi}_{n,\phi}\mathbf{W}) \le \overline{V_n}^2 \quad \forall \phi \in \mathcal{P}_n,\ n \in \mathcal{N} \quad (21)$$

$$\sum_{k=0,2,\cdots,K} V_{n,\phi}^{k^2} \le \alpha \mathbf{\Phi}_{n,\phi}\mathbf{W} \quad \forall n \in \mathcal{N},\ \phi \in \mathcal{P}_n \quad (22)$$

For the standard OPF problem, all constraints can be re-written in terms of $\mathbf{W}$. However, in the harmonic augmented problem the voltage variable $\mathbf{V}$ is present in FCM constraints (8) and (9). The voltage variable can be approximated from the values of the first coloum of $\mathbf{W}$, due to the slack bus convention $V_{0,a} = 1$ and $V_{0,a}^* V_{n,\phi} = V_{n,\phi}$. With these modifications, and by relaxing the rank 1 constraint of $\mathbf{W}$, the semidefinite relaxation of harmonic-constrained OPF **P1** is:

(P2)

$$\begin{aligned} \underset{\{\mathbf{P_G},\ \mathbf{Q_G},\ \mathbf{W},\mathbf{V},\ \mathbf{V_h},\ \mathbf{IG}\}}{\text{Minimize:}} \quad & C_0 = \sum_{s\in\mathcal{S}} c_s \sum_{\phi\in\mathcal{P}_s} P_{G,s,\phi} \\ \text{Subject to:} \quad & (20),(21),(17),(18) \\ & (8),(9),(15),(22) \\ & \mathbf{V} = \mathbf{W}\mathbf{e_1} \\ & \mathbf{W} \succeq 0 \end{aligned}$$

P2 is a semidefinite program and can be effectively solved using commercial solvers.

V. Numerical Result

In this section, we solve the harmonics-constrained OPF using CVX, a package for specifying and solving convex programs [18], [19], and MOSEK solver [20] for the following two networks:

- 10-bus unbalanced system as shown in Fig. 5; and
- the IEEE 13-bus test feeder [21] as shown in Fig. 8.

In both networks three-phase converters with parameters listed in Table II are included as distributed resources. The converter real power lower and upper limits are set to be from 0 kW and 300 kW, and the reactive power is regulated at 0 kVAR. The FCM is calculated according to [9] with maximum harmonic frequency order $K = 10$.

The line and load data for the IEEE 13-bus test feeder is adopted from [21] with the following modifications to remove the disconnect switch and other equipment not considered in the OPF formulation [11]:

- The transformer between bus 4 and 5 is replaced with a 500 ft. overhead line of Config. #602 overhead line;
- The disconnect switch between bus 2 and 8 is replaced with a 100 ft. underground line of Config. #606;
- Only the spot load are included, and all spot load are modeled as PQ type;
- the voltage supporing capacitors are not included.

For the 4.16 kV network of Fig. 5, the the lines are all set to be of Config. #601 from [21], and 0.2 mile in length. The loads at each bus are of three-phase type with value connected to each phase listed in Table III.

The cost of power supplied by the transmission network from Node 0 is set to \$40/MW, and the cost of power supplied by the distributed generations are set to be \$10/MW. The lower and upper limit for each bus voltage is set to be 95% and 105% of the nominal level. For each network, we solve a sequence of the problem with increasing values of the α parameter that constraints the maximum allowable voltage THD at each nodes. The simulation result for the 10-Bus network is shown in Fig. 6 and 7. The result for the IEEE 13-Bus feeder is shown in Fig. 9 and 10.

Even the rank 1 constraint is relaxed in the SDP, the solution $\mathbf{W}$ for both study case appears to have a single dominantly large eigenvalue. For the 10-bus network, when the THD allowance $\alpha = 1\%$, the two largest eigenvalues of solution $\mathbf{W}$ are $\lambda_1 = 518.07$ and $\lambda_2 = 0.0019$. When $\alpha = 20\%$, the two largest eigenvalues of $\mathbf{W}$ are $\lambda_1 = 518.83$ and $\lambda_2 = 0.0028$. For the IEEE 13-bus feeder, when the THD allowance $\alpha = 1\%$, the two largest eigenvalues of solution $\mathbf{W}$ are $\lambda_1 = 537.49$ and $\lambda_2 = 0.0007$. When $\alpha = 10\%$, the two largest eigenvalue of $\mathbf{W}$ are $\lambda_1 = 540.85$ and $\lambda_2 = 0.0009$.

The THD for each voltage is plotted with respect to the maximum allowable value α for the two test networks in Fig. 6 and 9. As the allowance for harmonic increases, the THD increases across the network for the 10-Bus feeder system but

TABLE II

CONVERTER PARAMETER LIST

$R_a = 0.02\ \Omega$	$R_b = 0.02\ \Omega$	$R_c = 0.02\ \Omega$
$L_a = 0.2\ H$	$L_b = 0.2\ H$	$L = 0.2\ H$
$C = 0.5\ F$	$\Omega = 377\ rad/sec$	

TABLE III

10-BUS TEST NETOWRK LOAD LIST

Load Data		
Bus	P(kW)	Q(kVAR)
1	50	20
3	130	82
4	130	82
5	110	60
6	110	60
8	90	30
9	90	30

remains under the allowable α value. For the IEEE 13-Bus feeder, it appears that the trend is less uniform, where the THD for some buses decrease with higher THD allowance. This implies the voltage THD at some buses can be reduced by allowing higher THD at other bus in the network.

The total cost of generation with respect to the increasing harmonics allowance α is shown as blue curve for both networks in Fig. 7 and 10 respectively. In addition, the power injected by the transmission network at the slack bus and the power generated by the distributed generators in the distribution network is also shown for each α value. As shown by these result, the reduction in cost is due to the increasing amount of cheaper DG generation that is enabled by allowing more harmonics.

VI. CONCLUSION

In this paper, we have formulated a harmonic-constrained OPF. The frequency coupling matrix is used to model the harmonics characteristic of individual converters in the network. The network voltage and current are modeled using

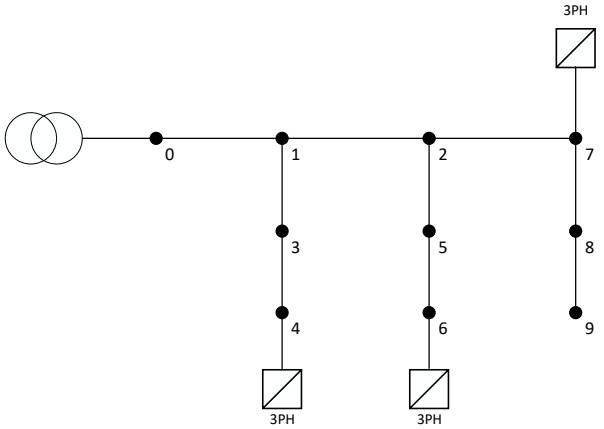

Fig. 5. A 10-Bus Test Network

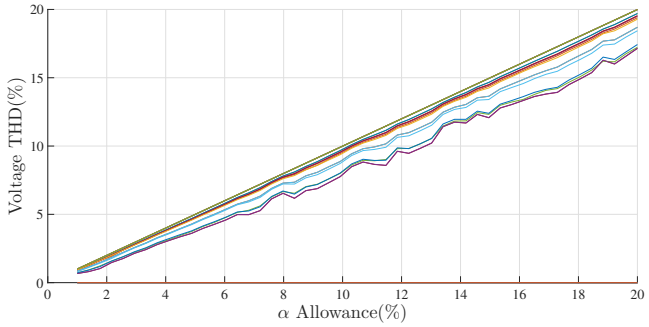

Fig. 6. Voltage THD vs. Increasing Allowance for 10-Bus Test System Each curve is the THD of one bus voltage

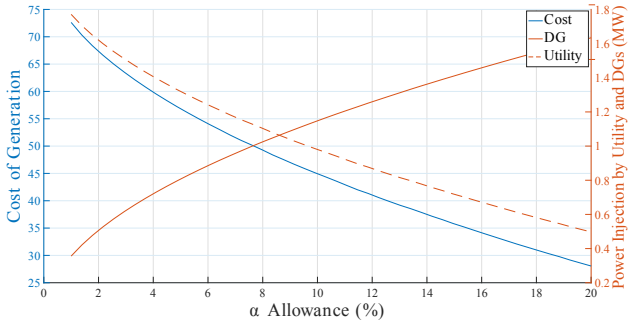

Fig. 7. Power Generation Cost and Portfolio vs. Increasing Allowance for 10-Bus Test System

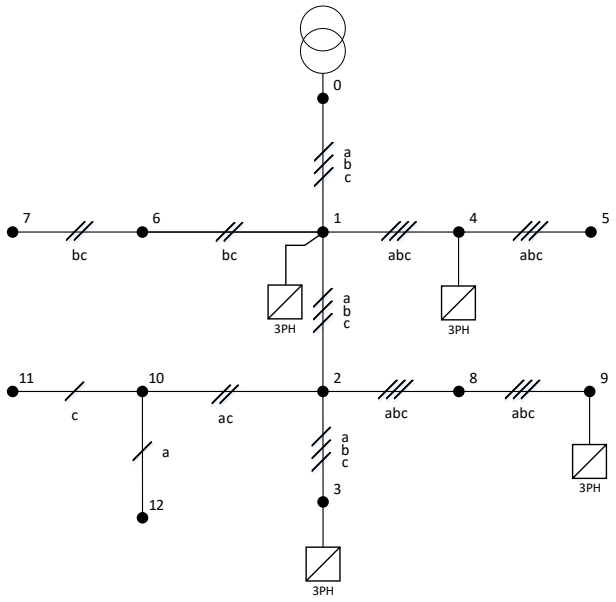

Fig. 8. IEEE 13-Bus Feeder Network

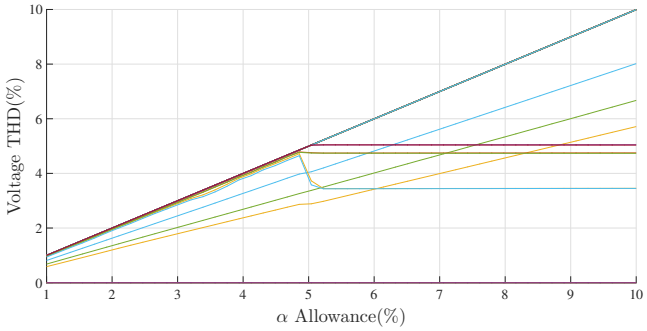

Fig. 9. Voltage THD vs. Increasing Allowance for IEEE 13-Bus Feeder Each curve is the THD of one bus voltage

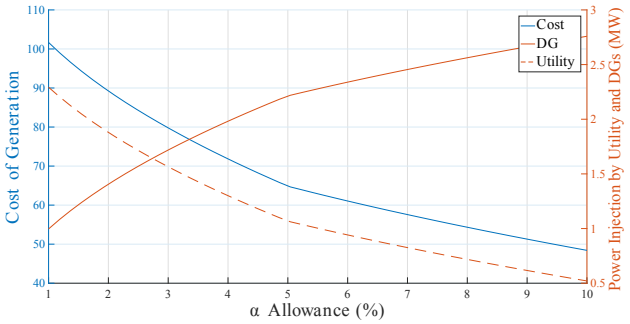

Fig. 10. Power Generation Cost and Portfolio vs. Increasing Allowance for IEEE 13-Bus Feeder

the modified system impedance at each harmonic frequency. The effect of harmonics is constrained by limiting the total harmonic distortion of each nodal voltage in the network. The non-convex optimization problem is relaxed using a semidefinite relaxation, and implemented for two test networks. The numerical results show that the method successfully capture the harmonics behavior in the network, and the OPF solution is influenced by restricting the maximum harmonics distortion in the network.

REFERENCES

[1] M. Shahidehpour and J. F. Clair, "A functional microgrid for enhancing reliability, sustainability, and energy efficiency," *The Electricity Journal*, vol. 25, no. 8, pp. 21–28, 2012. [Online]. Available: http://www.sciencedirect.com/science/article/pii/S1040619012002278

[2] N. Hatziargyriou, H. Asano, R. Iravani, and C. Marnay, "Microgrids," *IEEE Power and Energy Magazine*, vol. 5, no. 4, pp. 78–94, Jul. 2007.

[3] M. Huneault and F. D. Galiana, "A survey of the optimal power flow literature," *IEEE Transactions on Power Systems*, vol. 6, no. 2, pp. 762–770, May 1991.

[4] S. H. Low, "Convex Relaxation of Optimal Power Flow—Part I: Formulations and Equivalence," *IEEE Transactions on Control of Network Systems*, vol. 1, no. 1, pp. 15–27, Mar. 2014. [Online]. Available: http://ieeexplore.ieee.org/document/6756976/

[5] H. Sharma, M. Rylander, and D. Dorr, "Grid Impacts Due to Increased Penetration of Newer Harmonic Sources," *IEEE Transactions on Industry Applications*, vol. 52, no. 1, pp. 99–104, Jan. 2016.

[6] M. S. Rad, M. Kazerooni, M. J. Ghorbany, and H. Mokhtari, "Analysis of the grid harmonics and their impacts on distribution transformers," in *2012 IEEE Power and Energy Conference at Illinois*, Feb. 2012, pp. 1–5.

[7] Y. Sun, G. Zhang, W. Xu, and J. G. Mayordomo, "A Harmonically Coupled Admittance Matrix Model for AC/DC Converters," *IEEE Transactions on Power Systems*, vol. 22, no. 4, pp. 1574–1582, Nov. 2007.

[8] F. Yahyaie and P. W. Lehn, "Using Frequency Coupling Matrix Techniques for the Analysis of Harmonic Interactions," *IEEE Transactions on Power Delivery*, vol. 31, no. 1, pp. 112–121, Feb. 2016. [Online]. Available: http://ieeexplore.ieee.org/document/7119609/

[9] P. W. Lehn and K. L. Lian, "Frequency Coupling Matrix of a Voltage-Source Converter Derived From Piecewise Linear Differential Equations," *IEEE Transactions on Power Delivery*, vol. 22, no. 3, pp. 1603–1612, Jul. 2007. [Online]. Available: http://ieeexplore.ieee.org/document/4265685/

[10] X. Zong, P. A. Gray, and P. W. Lehn, "New Metric Recommended for IEEE Standard 1547 to Limit Harmonics Injected Into Distorted Grids," *IEEE Transactions on Power Delivery*, vol. 31, no. 3, pp. 963–972, Jun. 2016. [Online]. Available: http://ieeexplore.ieee.org/document/7042262/

[11] E. Dall'Anese, Hao Zhu, and G. B. Giannakis, "Distributed Optimal Power Flow for Smart Microgrids," *IEEE Transactions on Smart Grid*, vol. 4, no. 3, pp. 1464–1475, Sep. 2013. [Online]. Available: http://ieeexplore.ieee.org/document/6502290/

[12] W. H. Kersting, *Distribution System Modeling and Analysis, Third Edition.* Abingdon; Abingdon: CRC Press Taylor & Francis Group [distributor, 2012, oCLC: 895705799. [Online]. Available: http://www.crcnetbase.com/isbn/9781439856475

[13] R. W. Erickson and D. Maksimovic, *Fundamentals of power electronics*. New York: Springer Science + Business Media, 2004, oCLC: 264766903.

[14] M. Au and J. Milanovic, "Establishment of load composition in aggregate harmonic load model at LV buses based on field measurements," vol. 2005. IEEE, 2005, pp. v2–29–v2–29. [Online]. Available: http://digital-library.theiet.org/content/conferences/10.1049/cp˙20051024

[15] R. Burch, G. Chang, C. Hatziadoniu, M. Grady, Y. Liu, M. Marz, T. Ortmeyer, S. Ranade, P. Ribeiro, and W. Xu, "Impact of aggregate linear load modeling on harmonic analysis: a comparison of common practice and analytical models," *IEEE Transactions on Power Delivery*, vol. 18, no. 2, pp. 625–630, Apr. 2003. [Online]. Available: http://ieeexplore.ieee.org/document/1193887/

[16] K. R. Krishnanand, J. Moirangthem, S. Bhandari, and S. K. Panda, "Harmonic load modeling for smart microgrids." IEEE, Aug. 2015, pp. 68–72. [Online]. Available: http://ieeexplore.ieee.org/document/7435867/

[17] S. H. Low, "Convex Relaxation of Optimal Power Flow—Part II: Exactness," *IEEE Transactions on Control of Network Systems*, vol. 1, no. 2, pp. 177–189, Jun. 2014. [Online]. Available: http://ieeexplore.ieee.org/document/6815671/

[18] M. Grant and S. Boyd, "CVX: Matlab software for disciplined convex programming, version 2.1," http://cvxr.com/cvx, Mar. 2014.

[19] ——, "Graph implementations for nonsmooth convex programs," in *Recent Advances in Learning and Control*, ser. Lecture Notes in Control and Information Sciences, V. Blondel, S. Boyd, and H. Kimura, Eds. Springer-Verlag Limited, 2008, pp. 95–110, http://stanford.edu/ boyd/graph˙dcp.html.

[20] MOSEK Aps, *The MOSEK optimization toolbox for MATLAB manual. Version 7.0 (Revision 141).* , 2015. [Online]. Available: http://docs.mosek.com/7.0/toolbox/index.html

[21] W. Kersting, "Radial distribution test feeders," vol. 2. IEEE, 2001, pp. 908–912. [Online]. Available: http://ieeexplore.ieee.org/document/916993/